Available online at www.sciencedirect.com
ScienceDirect
Journal of Molecular Catalysis A: Chemical 261 (2007) 131–138
JOURNAL OF MOLECULAR CATALYSIS A: CHEMICAL
www.elsevier.com/locate/molcata

Photodegradation of dye pollutants on one-dimensional TiO_2 nanoparticles under UV and visible irradiation

Jingyi Li [a,b,*], Wanhong Ma [b], Chuncheng Chen [b], Jincai Zhao [b], Huaiyong Zhu [c], Xueping Gao [d]

[a] College of Chemistry and Chemical Engineering, Inner Mongolia University, Hohhot, Inner Mongolia 010021, China
[b] Centre for Molecular Science, Institute of Chemistry, The Chinese Academy of Science, Beijing 100080, China
[c] School of Physical and Chemical Sciences, Queensland University of Technology, GPO Box 2434, Brisbane, Qld 4001, Australia
[d] Institute of New Energy Material Chemistry, Nankai University, Tianjin 300071, China

Received 10 July 2005; received in revised form 10 March 2006; accepted 2 August 2006
Available online 7 September 2006

Abstract

Titanium dioxides (TiO_2) nanoparticles with one-dimensional (1D) geometry, nanorods and nanostripes, were used as photocatalysts to photodegrade Rhodamine B (RhB) under ultraviolet (UV) and visible irradiation. The nanorods catalyst exhibited very interesting photocatalytic properties: under the UV irradiation its catalytic activity was slightly below that of the well-known TiO_2 catalyst P25, while under visible light it exhibited a better activity than P25.

This fact indicates that the nanorods have a superior ability to utilize less energetic but more abundant visible light. Moreover, the 1D TiO_2 nanoparticles can be readily separated from aqueous suspensions by sedimentation after the reaction. With these advantages the 1D TiO_2 catalysts have a great potential for environmental applications. Various analytical techniques were employed to characterize TiO_2 catalysts and monitor the photocatalytic reaction. It was found that the catalytic performance of the catalysts is greatly dependent on their structures: The superior activity of P25 (consists of anatase and rutile nanocrystals) under UV light results probably from the interfacial interaction between anatase and rutile nanocrystals in this solid, which do not exist in the nanorods (only anatase). The titanate nanostripes (titanate) can absorb UV photons with shorter wavelength only.

Keywords: TiO_2 nanoparticles; RhB; UV and visible irradiation

1. Introduction

In the past three decades, the application of semiconductor heterogeneous photocatalysts in the photodegradation of toxic organic pollutants has been extensively investigated [1–6]. Titanium dioxides (TiO_2) are the most often used catalysts for such applications because they are non-toxic, relatively cheap, chemically stable throughout a wide pH range and robust under UV illumination. It is known that synthetic dyes released from their manufacturing and application processes, even at a low concentration (a few tens to a hundred parts per million), can cause serious water pollution [7–9]. These dyes are generally refractory (non-biodegradable) and cannot be removed from water via routine wastewater treatment process. Therefore, removal of the dyes from water by photocatalytic technique is an important environmental issue [7–14].

The degradation mechanism of the organic pollutants on TiO_2 under UV light is as follows [10]:

$$TiO_2 + h\nu \rightarrow e^- + h^+ \quad (1)$$

$$OH^- + h^+ \rightarrow {}^\bullet OH \quad (2)$$

$$H_2O + h^+ \rightarrow {}^\bullet OH + H^+ \quad (3)$$

$$O_2 + e^- \rightarrow {}^\bullet O_2{}^- \quad (4)$$

$${}^\bullet O_2{}^- + H^+ \rightarrow {}^\bullet OOH \quad (5)$$

The radicals formed in the above process are powerful oxidation agents, which oxidize the organic pollutants to carbon dioxide, water and other mineralized products. However, UV

* Corresponding author at: College of Chemistry and Chemical Engineering, Inner Mongolia University, Hohhot, Inner Mongolia 010021, China. Tel.: +86 471 4343236; fax: +86 471 4990101.
E-mail address: lijingyicn@yahoo.com (J. Li).

1381-1169/$ – see front matter © 2006 Elsevier B.V. All rights reserved.
doi:10.1016/j.molcata.2006.08.018

light in sunlight accounts for a small portion of the solar energy, only 3–5% of the overall energy of sunlight, and artificial UV light is expensive. It seriously limits the practical application of this photocatalytic reaction. Recently, we reported the photodegradation of dyes under visible light using TiO_2 [11–19]. The mechanism of such a degradation process is shown as follows:

$$\text{dye} + h\nu \rightarrow \text{dye}^* \quad (6)$$

$$\text{dye}^* + \text{TiO}_2 \rightarrow \text{dye}^{\bullet+} + \text{TiO}_2(\text{e}) \quad (7)$$

$$\text{TiO}_2(\text{e}) + \text{O}_2 \rightarrow \text{TiO}_2 + \text{O}_2^{\bullet-} \quad (8)$$

$$\text{O}_2^{\bullet-} + \text{TiO}_2(\text{e}) + 2\text{H}^+ \rightarrow \text{H}_2\text{O}_2 \quad (9)$$

$$\text{H}_2\text{O}_2 + \text{TiO}_2(\text{e}) \rightarrow \text{OH}^{\bullet} + \text{OH}^- \quad (10)$$

$$\text{dye}^{\bullet+} + \text{O}_2(\text{or}\text{O}_2^{\bullet-}\text{or}^{\bullet}\text{OH}) \rightarrow \text{peroxylatedorhydroxylatedintermediates} \rightarrow\rightarrow \text{degradedormineralizedproducts} \quad (11)$$

Such a process is of significance for both fundamental and practical studies because of the special mechanism and the perspective in treatment of dye pollutants under sunlight, respectively. Besides, for the photocatalysis processes in which fine TiO_2 powders are used as catalysts, an important issue is to recover fine TiO_2 powders from aqueous suspensions. Since the photocatalytic reactions take place on the catalyst surface, the catalysts with a large specific surface area are expected to have high catalytic activities. Nanoparticles have significant advantages in these applications because of their small and uniform particle size and large surface area. But it is extremely difficult to recover the fine TiO_2 powders from water, leading to a potential difficulty in downstream separation. Continuing efforts has been made to synthesize the TiO_2 structures which can be separated readily, and exhibit superior catalytic performance. For example, we used composite catalysts of anatase nanocrystals and layered clays to degrade sulforhodamine (SRB) and found that they exhibited a good catalytic activity and were easy to sediment from aqueous suspensions [13,14].

In the present study, we used novel TiO_2 nanorods and TiO_2 nanostripes as photocatalysts to degrade Rhodamine B under UV and visible light irradiation. The catalytic performance of the 1D-nanoparticle catalysts was compared with that of P25, the well-known photocatalyst of titanium dioxide fine powder from Degussa AG, Germany. TiO_2 nanorods have large BET specific surface areas and regular morphology on nanometer scale. Due to their 1D morphology, the nanorods sediment readily from aqueous dispersions, compared to P25, and thus they are easy to be separated for reuse. Absorption spectra, chemical oxygen demand (COD_{Cr}), total organic carbon (TOC) and electron paramagnetic resonance (EPR) spetroscopies were employed to monitor the photooxidation process of RhB. The TiO_2 catalysts were characterized by UV–vis diffuse reflectance spectra, Raman spectra, surface photovoltage spectra (SPS), X-ray diffraction (XRD) and transmission electron microscope (TEM). The results provide us useful information for understanding the relation between the structure and catalytic properties of the 1D TiO_2 nanoparticles.

2. Experimental section

2.1. Materials

Commercial titania powder of P25 was kindly supplied by Degussa AG Germany, which contains about 80% of anatase and 20% of rutile and has a BET specific surface area of about 50 $m^2\,g^{-1}$. The TiO_2 nanorod catalysts were prepared from titanium hydroxide precipitate, which was obtained from $TiCl_4$ as described in literature [20,21]. Briefly, the fresh titanium hydroxide and 15 M NaOH solutions were mixed and transferred into an autoclave and kept at 110 °C for 48 h. The obtained white solids were recovered by centrifugation and washed with deionised water for three times, 0.1 M HCl solution once, and finally with distilled water until a pH value about 7 was reached. In the washing process the wet cake was dispersed into 100 ml of water (or acid solution) whilst stirring and then the solid was recovered by centrifugation. The samples were dried at 110 °C for one day and then calcined at 400 °C for 3 h in air. The TiO_2 nanostripes were prepared under the same procedure but using P25 as the starting material to react with NaOH solution. The BET specific surface area of the calcined nanorods and nanostripes are 314 and 469 m^2/g, respectively, and the pore volumes are 1.51 and 3.37 cm^3/g, respectively.

The 5,5-dimethyl-1-pyrroline-*N*-oxide (DMPO) was purchased from the Sigma Chemical Co. Rhodamine B (RhB, its structure is shown below.) and other chemicals involved in this study were analytical reagent grade and were used without further purification. Deionized and doubly distilled water was used throughout this study. The pH of aqueous solutions was adjusted by diluted NaOH or $HClO_4$ aqueous solutions.

2.2. Photoreactor and light source

The UV resource was a 100 W Hg lamp ($\lambda > 330$ nm, Toshiba SHLS-1002A). A 500 W halogen lamp (Institute of Electric Light Source, Beijing), used as visible light source, was positioned inside a cylindrical Pyrex glass vessel surrounded by a circulating water jacket of Pyrex glass to cool the lamp. A cut-off filter was placed outside the Pyrex jacket to completely filter out the light with wavelengths shorter than 410 nm and to ensure that the irradiation entering the reaction system was visible light only.

2.3. Procedures and analyses

An aqueous dispersion of TiO_2 catalyst and RhB dye was prepared for the photocatalytic test by dispersing 25 mg of TiO_2 powder to a 25 ml solution containing the RhB at given concentrations. This reaction dispersion was magnetically stirred in the dark for ca. 30 min prior to irradiation to establish the adsorption/desorption equilibrium of the dye on the catalyst surface. At given irradiation time intervals, specimens (4 ml) were taken from the dispersion, centrifuged, and subsequently filtered

through a Millipore filter (pore size, 0.22 μm) to separate the TiO_2 particles. The filtrates were analyzed by UV–vis spectra with a shimadzu-160 A spectrophotometer. Chemical oxygen demand (COD) of the dispersions was measured by the dichromate titration method [22] (referred to as COD_{Cr}). Total organic carbon (TOC) of the filtrates was determined by TOC analyzer (Tekmar dohrmann Apollo 9000). Electron paramagnetic resonance signals of radicals spin-trapped by DMPO were recorded on a Brucker EPR 300E spectrometer [23,24]. The settings for EPR were: center field 3480 G, sweep width 100 G, modulation frequency 100 KHz and power 10.02 mW. Raman spectra were measured with Renishaw 2000 spectrograph. Surface photovoltage spectra (SPS) were recorded with a homemade SPS measurement system. X-ray diffraction (XRD) was measured on Rigaka D/max-2500 using Cu Kα radiation and a fixed power source (45 kV, 300 mA). The powder samples were scanned at a rate of 1° (2θ)/min over a range of 2–80°. The microstructure and morphology of the samples were examined using a transmission electron microscope (FEI Tecnai 20) with the acceleration voltage of 200 kV.

3. Results and discussion

3.1. The degradation of RhB

The changes in the concentration of RhB under UV and visible irradiation in aqueous TiO_2 nanorod dispersions are shown in Figs. 1 and 2, respectively. The adsorption of dye (the initial concentration of 2×10^{-5} M) on the catalysts was about 10–14%. The absorption band of RhB at 554 nm decreased rapidly under both UV and visible irradiations and had a slight blue shift (see Fig. 1 inset), indicating the formation (or presence) of some *N*-de-ethylated intermediates during the photocatalytic oxidation of RhB. Similar phenomenon was observed in the SRB/TiO_2 system [11,12].

From the results shown in Fig. 1 one can derive the rate constants of a pseudo-first-order reaction. For P25 and TiO_2 nanorods under UV irradiation, the constants are 3.72×10^{-2} and 2.64×10^{-2} min^{-1}, respectively. The pseudo-zero-order rate constant was 6.84×10^{-3} M min^{-1} when TiO_2 nanostripe was used as a catalyst under the otherwise identical conditions. The degradation rate on TiO_2 nanorods is slightly lower than that on P25, while the degradation on TiO_2 nanostripes is substantially slow, compared with those on the TiO_2 nanorods and P25 catalysts under UV irradiation. There are several reasons for this phenomenon. One reason is the amount of •OH produced on TiO_2 nanostripes is relatively low under UV irradiation (according to the EPR spectral assays in Section 3.2). The •OH radicals are the oxidation agent, which oxidizes organic compounds [7–10]. Besides, the recombination of e^- and h^+ on TiO_2 nanostripes could be much faster than that on P25 and the nanorod. Blank experiments show that the degradation of RhB was negligible without UV irradiation or in the absence of catalysts.

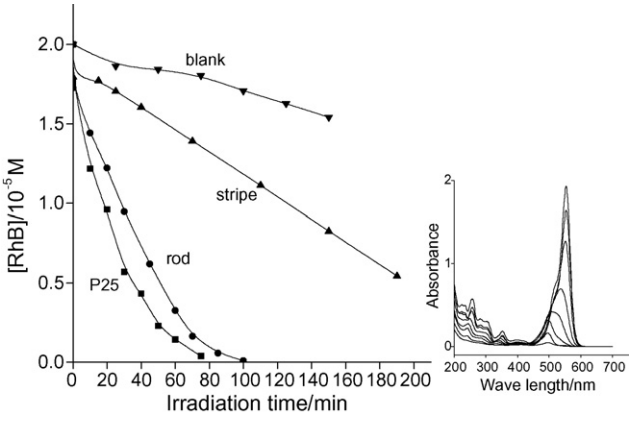

Fig. 1. RhB concentration decreases with UV irradiation time. Inset figure: UV–vis spectra of RhB (2×10^{-5} M, 25 ml, pH 3.5) in aqueous TiO_2 nanorod dispersions at different intervals of the irradiation time. Spectra from the top to the bottom refer to before addition of TiO_2 nanorod particles; equilibrium established after addition of TiO_2 nanorod particles (1 g/l); irradiation for 10, 20, 30, 45, 70, 100 min, respectively.

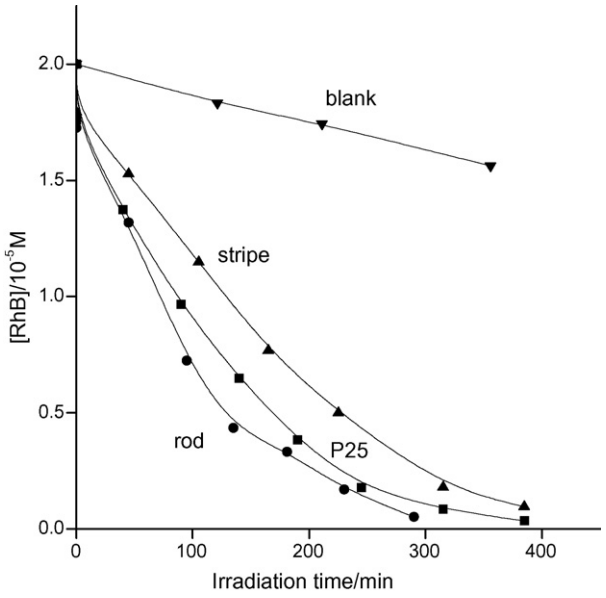

Fig. 2. RhB concentration decreases with irradiation time under visible light irradiation.

Under visible light irradiation, the pseudo-first-order rate constants for the photodegradation of RhB are 7.90×10^{-3}, 9.49×10^{-3} and 6.43×10^{-3} min^{-1} when P25, TiO_2 nanorods and TiO_2 nanostripes were used as catalysts, respectively (Fig. 2). The dye degradation under visible light was obviously slower than that under UV light for all the three catalysts. However, the degradation rate achieved by the TiO_2 nanorods was about 36% of the rate achieved by this catalyst under UV light, while the degradation rate on P25 under visible light was only 21% of the rate on the same catalyst under UV light. This leads to interesting fact that under visible light the dye degradation on TiO_2 nanorods is the fastest. Moreover, the nanorod catalyst was much easier to be separated from solutions compared to P25. The nanorods sedimentated from an aqueous suspension in an hour. In contrast, the aqueous suspensions of P25 were unclear after several hours. This is a profound advantage when the catalyst is used in practice because separating ultra-fine catalyst powders has serious problem, which impeded the applications

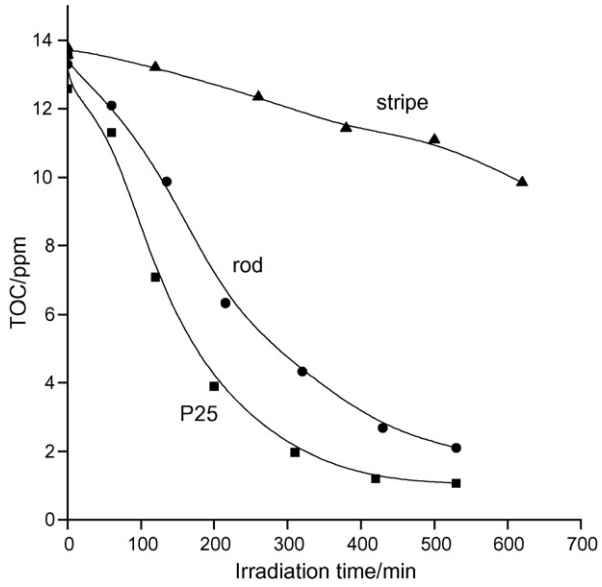

Fig. 3. TOC changes in the course of the photocatalytic degradation of RhB (4×10^{-5} mol/L, 100 mL) in the presence of catalysts (100 mg) at pH 3.5 under UV irradiation.

of TiO_2 photocatalysts at industrial scale [9]. Blank experiments indicate that RhB did not degrade in catalyst suspensions in the dark, and the degradation of RhB under UV irradiation was negligible in the absence of catalysts.

Why do P25 particles show almost the same dye degradation performance under UV light as nanorods in the light of the fact that the surface area of the latter has an additional contribution to dye degradation under the visible light irradiation? We should consider their different reaction mechanisms. Under visible light irradiation, electrons transfer from the excited dye to the conduction band of TiO_2. A bigger BET surface area and a stronger adsorption of dye are a necessary condition to finish this process so that nanorods have a better reaction activity than P25. Under UV light irradiation, TiO_2 is excited to produce electron and hole pairs. The recombination of electron and hole pairs and the reaction rate of interface decide the reaction efficiency. The recombination of electron and hole pairs of P25 is less likely than nanorods so that the reaction activity of P25 is better than nanorods.

The changes of COD could also reflect the extent of the degradation reaction of the dye. Under UV irradiation, the COD variation values for the irradiated RhB/catalysts suspensions were 62%, 22% and 77% for P25, TiO_2 nanostripes and TiO_2 nanorods within 180 min of irradiation, respectively. Under visible irradiation, the COD variation values were 31% and 30% within 720 min for P25 and TiO_2 nanostripes, respectively. This value for the TiO_2 nanorods was 68% indicating a much faster

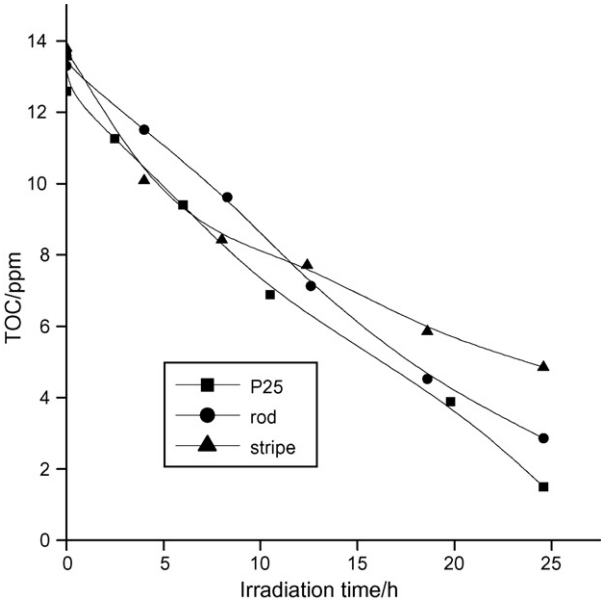

Fig. 4. TOC changes in the course of the photocatalytic degradation of RhB (4×10^{-5} mol/L, 100 mL) in the presence of catalysts (100 mg) at pH 3.5 under visible light.

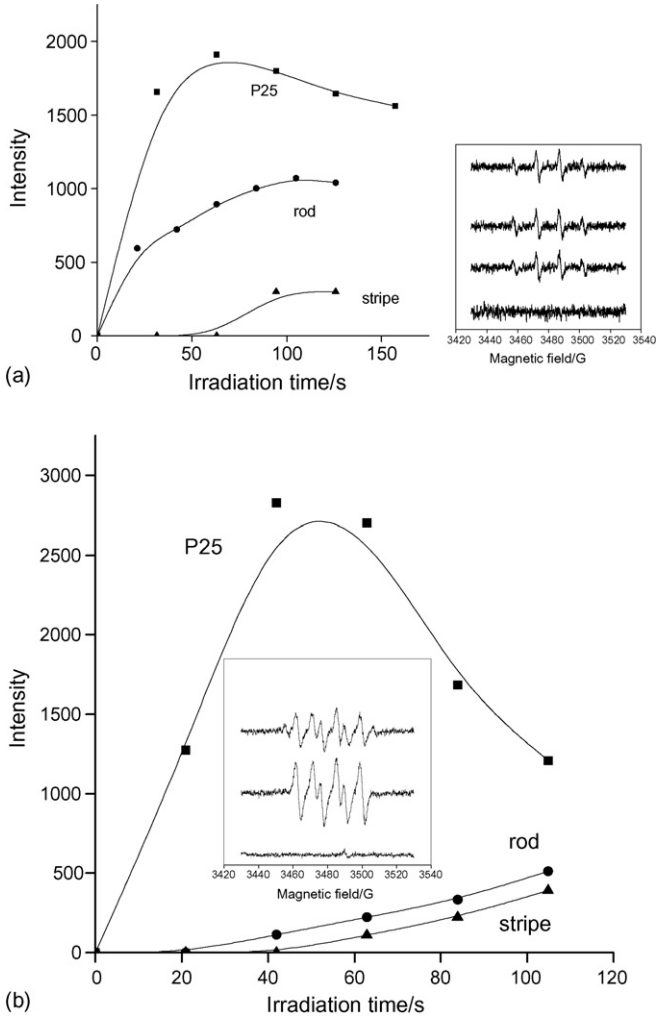

Fig. 5. (a) The intensities of hydroxyl radical signals under UV irradiation. The inset figure is the hydroxyl radical EPR spectra of TiO_2 nanorod/RhB system under UV irradiation (355 nm laser). The reaction conditions were pH 3.5 [RhB] = 4×10^{-5} M. (b) The intensities of peroxide radical signals under UV irradiation. The inset figure is the EPR spectra of peroxide radical in the TiO_2 nanorod system under UV irradiation (355 nm laser). The reaction condition is [RhB] = 4×10^{-5} M.

mineralization on the nanorods than that on P25 and TiO_2 nanostripes.

Decreases in TOC can also reveal the extent of the dye degradation in the photocatalysis systems. The TOC changes under UV and visible irradiation are shown in Figs. 3 and 4, respectively. Under UV irradiation, TOC values decrease to 1.1, 2.1 and 10.9 ppm by P25, TiO_2 nanorods and TiO_2 nanostripes, respectively, from about 13 ppm within 530 min of irradiation. These results are consistent with the kinetic data. Under visible irradiation, the pseudo-zero-order rate constants for the degradation of RhB were 0.438 and 0.439 h^{-1} ppm when using P25 and TiO_2 nanorods as catalysts, respectively, and TOC values decreased to 1.8 ppm and 3 ppm after irradiation of 25 h. The pseudo-first-order rate constant for the degradation of RhB was 0.0958 h^{-1} for TiO_2 nanostripes, being substantially smaller than those on the other two catalysts.

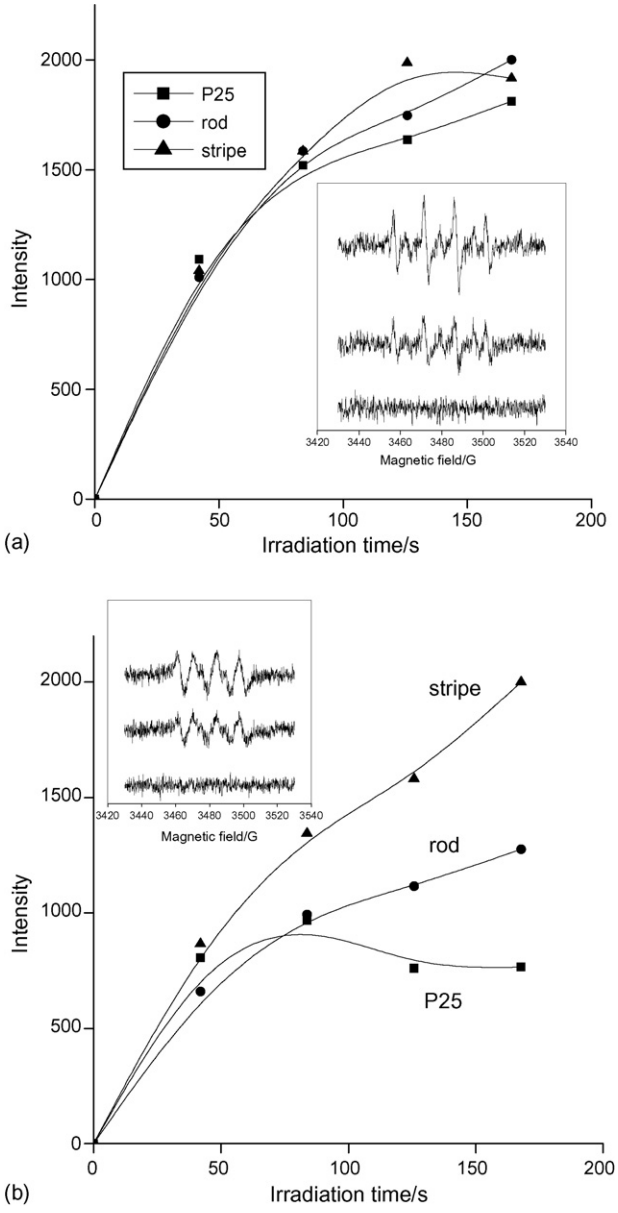

Fig. 6. (a) The intensities of hydroxyl radical signals under visible light irradiation. Inset figure is the hydroxyl radical EPR spectra of TiO_2 nanorod/RhB system under visible light irradiation, 532 nm laser. The reaction conditions are pH 3.5 [RhB] = 4×10^{-5} M. (b) The intensities of peroxide radical signals under visible light irradiation. Inset figure is the EPR spectra of peroxide radical in the TiO_2 nanorod/SRB system under visible irradiation (532 nm laser). The reaction condition is in [RhB] = 4×10^{-5} M.

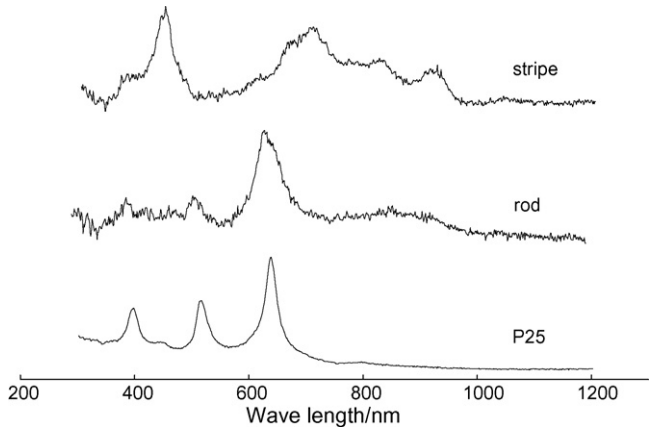

Fig. 7. Raman spectra of TiO_2.

3.2. EPR spectral assays

The EPR spectra under UV irradiation are shown in Fig. 5. No signals were detected without irradiation. However, the characteristic DMPO–•OH adducts with 1:2:2:1 quartet patterns [25] appeared in the presence of photocatalysts under UV irradiation (seen in Fig. 5a). P25 produced the largest amount of •OH, while TiO_2 nanostripes produced the least. DMPO–$O_2^{\bullet -}$ adducts with six characteristic peaks [26] can be obtained in methanol solvent (inset in Fig. 5b). P25 produced large amount of $O_2^{\bullet -}$, while the other two catalysts produced small amounts of these species. •OH and $O_2^{\bullet -}$ are active species for the photooxidation of dyes so that the amount of •OH radicals produced by the catalysts is crucial to their catalytic performance. Therefore, it is anticipated that the degradation rate of P25 is the fastest under UV irradiation.

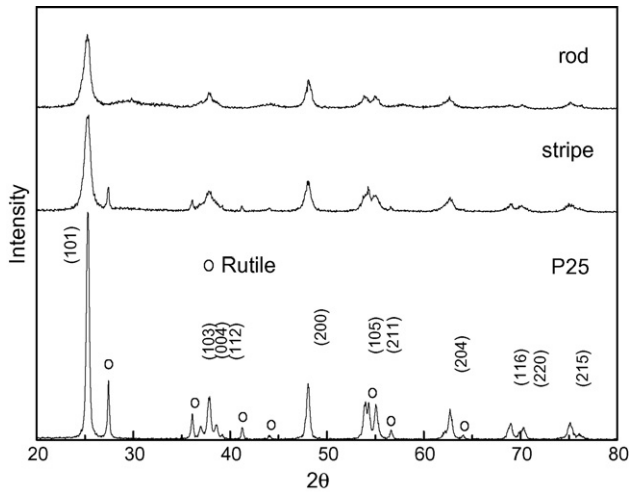

Fig. 8. XRD patterns of TiO_2.

Both DMPO–•OH and DMPO–$O_2^{\bullet-}$ were observed in the visible irradiation of the RhB/catalyst dispersion (Fig. 6). There are two classes of EPR peaks in Fig. 6a: one is due to DMPO–•OH, and the other is due to DMPO–•H. This is in agreement with the previous studies [27–29]. The systems of three different catalysts produce similar amounts of •OH (Fig. 6a). TiO_2 nanostripes produced the largest amount of $O_2^{\bullet-}$, while the smallest amount of $O_2^{\bullet-}$ was produced by P25.

3.3. Raman, XRD and TEM results

The Raman spectra of the samples are depicted in Fig. 7. The Raman peaks of anatase and rutile have been well documented [30], and thus the Raman spectra of the samples can provide information of the crystal phases in the samples. The peaks of anatase phase can be observed in the Raman spectra of P25 and TiO_2 nanorods, which consist mainly of anatase nanocrystals. But TiO_2 nanostripes were neither anatase nor rutile but a sort of titanate. These conclusions are supported by XRD results of the samples (Fig. 8). The difference in structure could be the reason for TiO_2 nanostripes exhibited slowest the degradation rate under UV irradiation. The nanorods we obtained had diameter of ca. 3–5 nm and lengths of ca. 20–40 nm. The nanostripes were about 10 nm wide and over 100 nm long (Fig. 9). Both are different from P25, which are particles with a diameter about 30–50 nm.

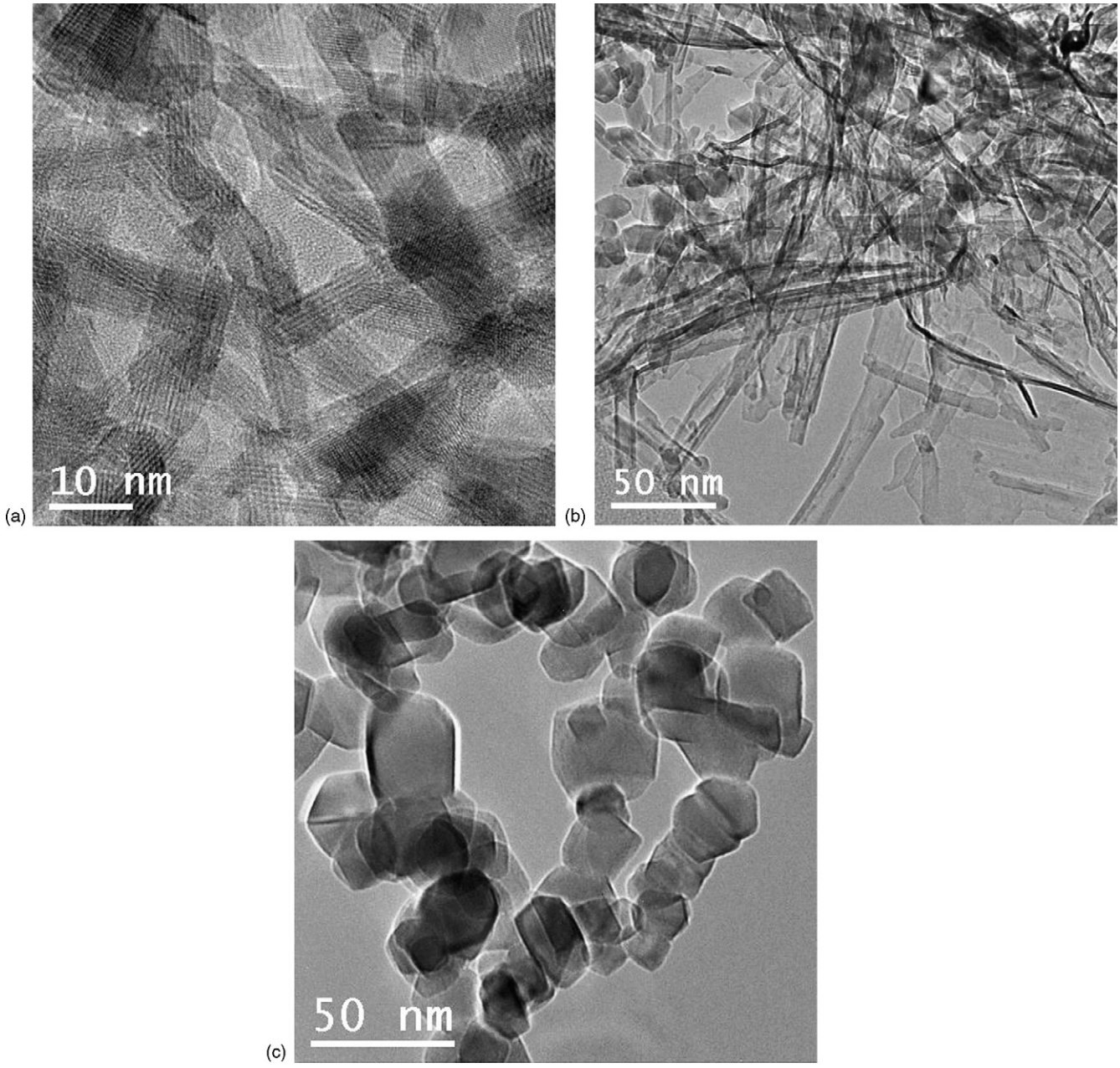

Fig. 9. TEM images of TiO_2: (a) nanorods; (b) nanostripes; (c) P25.

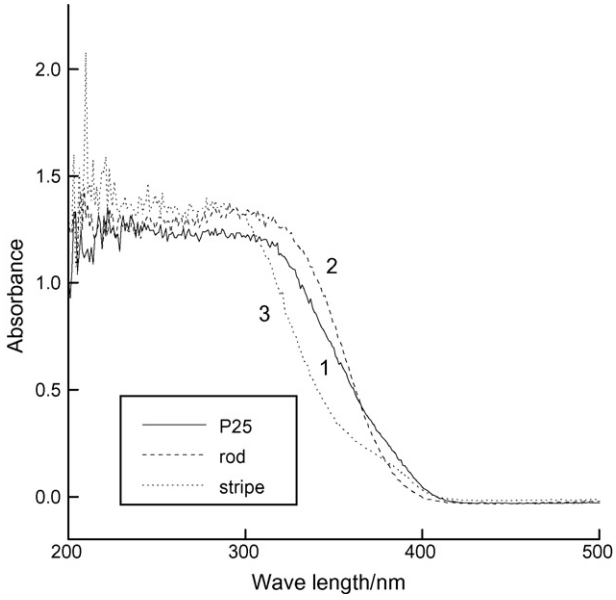

Fig. 10. UV–vis diffuse reflectance spectra of TiO_2. Curves 1–3 denote P25, TiO_2 nanorod and TiO_2 nanostripe, respectively.

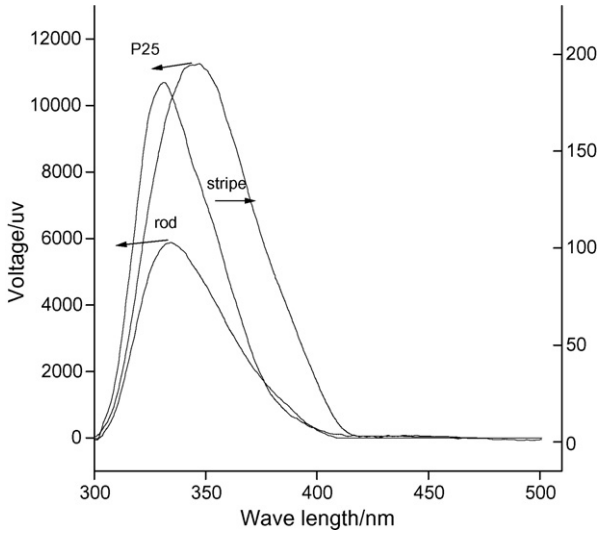

Fig. 11. Surface photovoltage spectra (SPS) of TiO_2.

3.4. UV–vis diffuse reflectance spectra

UV–vis diffuse reflectance spectra of the catalysts are shown in Fig. 10. Both 1D-nanoparticle catalysts had a slight blue shift, compared to P25.This blue shift can be attributed to the fact that the anatase crystal size in 1D-nanorods is smaller than that in P25. The decrease in the size of semiconductor crystals at a scale of 10 nm or below causes increase in the band gap of the crystals [31]. The TiO_2 nanorod sample has a large specific surface area (314 m^2/g) and a small crystalize size of anatase. Because the photocatalytic reaction takes place on the surface of the catalysts. Therefore, the TiO_2 nanorod sample has a larger anatase surface available for the degradation reaction, and it should exhibit superior photocatalytic activity under visible light irradiation.

3.5. Surface photovoltage spectra (SPS) results

A blue shift can be observed for TiO_2 nanorods and nanostripes in relative to that for P25, and the peak intensity of the two samples is smaller than that for P25 (Fig. 11). These results imply that larger energy is required for exciting TiO_2 nanorods and nanostripes than exciting P25. In other word, the photons with shorter wavelength can activate the degradation. The photoresponse of P25 was stronger than that of TiO_2 nanorods and nanostripes as the spectra illustrated. The results suggest that under identical UV irradiation more excited electrons and holes are generated on P25 than on the other two catalysts. Therefore, the photocatalytic activity of TiO_2 nanorods and nanostripes is lower than that of P25 under UV irradiation. The difference in photoresponse between the three materials could be attributed to their difference in crystal phases in the samples. P25 contains about 80% of anatase and 20% of rutile, nanorods are anatase and nanostripes are titanate. Anatase is generally regarded as the most active for the photocatalysis among the TiO_2 polymorphs [9,32], however, this argument could not provide convincing interpretation to our results in this study. Recently, it has been suggested that the interfaces between nanocrystals of different phases could make a very large contribution to the catalytic activity [33]. It appears that the interfaces between anatase and rutile nanocrystals in P25 result in the strong photoresponse and thus the better catalytic performance under UV light. The anatase nanorod sample has a large specific surface area but not such interfaces, while nanostripes are titanate, which absorb light of short wavelength as illustrated in Fig. 10.

4. Conclusions

TiO_2 nanoparticles with one-dimensional (1D) geometry are effective catalysts for photodegrading Rhodamine B (RhB) under both ultraviolet (UV) and visible light irradiation. In particular, the nanorods catalyst exhibit an performance even better than that of the well-known TiO_2 photocatalyst P25 under visible light. This is an important property, which allows to utilize less energetic but more abundant visible light. The photodegradation of the dye under visible light follows the mechanism we previously proposed [7–10]. These radicals are oxidation agent, which oxidizes the dye to CO_2, H_2O and mineral substances. In addition, the 1D dimension of the nanoparticles has an important advantage in the separation after reaction. These advantages greatly enhance potential of the catalyst for environmental applications. Under UV irradiation, the catalytic activity of the anatase nanorods is slightly below that of P25, and the activity of the titanate nanostripes is substantial lower. This can be attributed to the crystal phase and the interface between the nanocrystals of the catalysts. The anatase nanorods have a large surface area but no interfaces between anatase and rutile nanocrystals which could be response for the strong photoresponse observed in surface photovoltage spectra results, and thus for the superior catalytic activity under UV irradiation. The titanate nanostripes can absorb UV photons with higher energy (shorter wavelength) only. This study illustrates

that the structure and morphology of the TiO_2 nanoparticles have important effect on their catalytic performance and the results are useful for the design of new TiO_2 photocatalysts.

Acknowledgements

This work is supported financially by NSFC (Nos. 20133010, 4001161947, 20077027, 20567002 and 90206043) and CAS. Financial supports from the Australian Research Council (ARC) are also gratefully acknowledged, and H.Y.Z. is indebted to ARC for the QE II fellowship. This work is also supported financially by Scientific Research Startup Fund of Inner Mongolia University (203044), the Education Department of Inner Mongolia Autonomous Region (NJ04093 and NJ03121), Chunhui Plan of the Education Ministry (Z2004-2-15030) and "513 talents" Plan of Inner Mongolia University. We are also grateful to Prof. J.R. Chen and Dr. Z.Y. Tian for measurements of EPR and SPS spectra.

References

[1] S.N. Frank, A.J. Bard, J. Am. Chem. Soc. 99 (1977) 303.
[2] K.T. Ranjit, I. Willner, S.H. Bossmann, A.M. Braun, J. Catal. 204 (2001) 305.
[3] L. Cao, A. Huang, F. Spiess, S.L. Suib, J. Catal. 188 (1999) 48.
[4] Y.T. Kwon, K.Y. Song, W.I. Lee, G.J. Choi, Y.R. Do, J. Catal. 191 (2000) 192.
[5] L. Davydov, P.G. Smirniotis, J. Catal. 191 (2000) 105.
[6] L. Davydov, E.P. Reddy, P. France, P.G. Smirrniotis, J. Catal. 203 (2001) 157.
[7] O. Legrini, E. Oliveros, A.M. Braun, Chem. Rev. 93 (1993) 671.
[8] M.A. Fox, M.T. Dulay, Chem. Rev. 93 (1993) 341.
[9] M.R. Hoffmann, S.T. Martin, W. Choi, D.W. Bahnemann, Chem. Rev. 95 (1995) 69.
[10] H. Hidaka, J. Zhao, E. Pelizzetti, N. Serpone, J. Phys. Chem. 96 (1992) 2226.
[11] C. Chen, X. Li, W. Ma, J. Zhao, H. Hidaka, N. Serpone, J. Phys. Chem. B 106 (2002) 318.
[12] W. Zhao, C. Chen, X. Li, J. Zhao, H. Hidaka, N. Serpone, J. Phys. Chem. B 106 (2002) 5022.
[13] J. Li, C. Chen, J. Zhao, H. Zhu, J. Orthman, Appl. Catal. B 37 (2002) 331.
[14] J. Li, C. Chen, J. Zhao, H. Zhu, D. Zhe, Sci. China B 45 (2002) 445.
[15] G. Liu, X. Li, J. Zhao, H. Hidaka, N. Serpone, Environ. Sci. Technol. 34 (2000) 3982.
[16] G. Liu, X. Li, J. Zhao, S. Horikoshi, H. Hidaka, J. Mol. Catal. 153 (2000) 221.
[17] G. Liu, J. Zhao, H. Hidaka, J. Photochem. Photobiol. A 133 (2000) 83.
[18] T. Wu, G. Liu, J. Zhao, H. Hidaka, N. Serpone, New J. Chem. 24 (2000) 93.
[19] G. Liu, J. Zhao, New J. Chem. 24 (2000) 411.
[20] J. Ovenstone, K. Yanagisawa, Chem. Mater. 11 (1999) 2770.
[21] X.P. Gao, H.Y. Zhu, G.L. Pan, S.H. Ye, Y. Lan, F. Wu, D.Y. Song, J. Phys. Chem. B 108 (2004) 2868.
[22] Chinese National Standard. GB 11914-89; 1989.
[23] H. Noda, K. Oikawa, H. Kamada, Bull. Chem. Soc. Jpn. 65 (1992) 2505.
[24] H. Noda, K. Oikawa, H. Nishiguchi, H. Kamada, Bull. Chem. Soc. Jpn. 66 (1993) 3542.
[25] W.G. Wamer, J.J. Yin, R.R. Wei, Free Radical Biol. Med. 23 (1997) 851.
[26] J.R. Harbour, M.L. Hair, J. Phys. Chem. 82 (1978) 1397.
[27] A.S.W. Li, C.F. Chignell, J. Biochem. Biophys. Meth. 22 (1991) 83.
[28] C.F. Chignell, A.G. Motten, R.H. Sik, C.E. Parker, K. Reszka, J. Photochem. Photobiol. 59 (1994) 5.
[29] F.P. Sargent, E.M. Gardy, Can. J. Chem. 52 (1974) 3645.
[30] J.C. Parker, R.W. Siegel, J. Mater. Res. 5 (1990) 1246.
[31] M.L. Steigerwald, L.E. Brus, Acc. Chem. Res. 23 (1990) 183.
[32] A. Fujishima, K. Hashimoto, T. Watanabe, TiO_2 Photocatalysis Fundamentals and Applications, BKC, Inc., Tokyo, 1999.
[33] A.G. Agrios, K.A. Gray, E. Weitz, Langmuir 19 (2003) 1402.